



Intra-scenario variability of trends and controls of near-bed oxygen concentration on the Northwest European Continental Shelf under climate change

Giovanni Galli¹, Sarah Wakelin², James Harle³, Jason Holt², Yuri Artioli¹

5 ¹Plymouth Marine Laboratory (PML), Prospect Place, Plymouth, Devon, PL1 3DH, United Kingdom

²National Oceanography Centre (NOC), Joseph Proudman Building, 6 Brownlow Street, Liverpool, L3 5DA, United Kingdom

³National Oceanography Centre (NOC), European Way, Southampton, SO14 3ZH, United Kingdom

Correspondence to: Giovanni Galli (gig@pml.ac.uk)

10

15

20

25

30



Abstract. We present an analysis of the evolution of near-bed oxygen in the next century in the Northwest European Continental Shelf in a three-member ensemble of coupled physics-biogeochemistry models. The comparison between model results helps highlighting the biogeochemical mechanisms responsible for the observed deoxygenation trends and their response to climate drivers.

35 While all models predict a decrease in near bed oxygen proportional to climate change intensity, the response is spatially heterogeneous, with hotspots of oxygen decline in the members with the most intense change, as well as areas where compensating mechanisms mitigate change.

We separate the components of oxygen change associated to the warming effect on oxygen solubility from those due to the effects of changes in transport and ecosystem processes. We find that while warming is responsible for a mostly uniform
40 decline throughout the shelf, changes in transport and ecosystem processes account for the detected heterogeneity.

Hotspots of deoxygenation are associated with enhanced stratification that greatly reduces vertical transport. A major change in circulation in the North Sea is responsible for the onset of one such hotspot in the members characterised by intense climate change.

Conversely, relatively shallow and well mixed coastal areas in the south experience an increase in net primary production
45 that partially mitigates oxygen decline in all members.

This work represents the first multi-model comparison addressing deoxygenation in the Northwest European Shelf and contributes to the understanding of the processes that drive deoxygenation in continental shelf ecosystems.

50

55



1 Introduction

60 Oxygen availability is of vital importance for aquatic life and the occurrence of low oxygen concentrations represents a major threat for marine (and freshwater) ecosystems. Bindoff et al. (2019) estimated that the world's marine oxygen inventory has been declining by $1.55 \pm 0.88\%$ over the 1970-2010 period and a further decline of 3.45% compared to the 1990s is projected by the end of the century (Bopp et al., 2013) under the RCP8.5 scenario. A more recent estimate based on a CMIP5 and CMIP6 multi-model comparison estimated a global reduction of 9.51 to 13.27 mmol/m³ (under RCP8.5 and 65 SSP5-8.5 scenarios respectively) over the subsurface layer (100-600m) for the end of the century compared to pre-industrial values (Kwiatkowski et al., 2020).

Ocean oxygen concentration is determined by multiple complex processes. Air-sea gas exchange supplies oxygen to the upper ocean layers and primary production by phytoplankton contributes to a net production of oxygen in the euphotic layer, whilst away from the euphotic zone respiration exceeds primary production, resulting in net oxygen consumption. As 70 organic matter (from marine primary/secondary production and of terrestrial origin) sinks, it is consumed by bacteria and zooplankton that consume oxygen in the process. Mixing and ocean currents are responsible for delivering oxygen to the deeper layers and where the ocean is stratified (either permanently or seasonally) the transport of oxygen from the surface to the bottom layer is inhibited. In addition to that, oxygen solubility is controlled by temperature (and salinity), hence ocean warming will limit the amount of oxygen that can be dissolved in seawater.

75 The bottom layer of the oceans is especially vulnerable to oxygen depletion because it is isolated from the surface and possibly from the euphotic layer, and because sinking organic matter may accumulate there and be respired by bacteria and other organisms. In fact, in the global ocean, oxygen minimum zones are generally found in subsurface waters where high surface productivity and associated high respiratory demand are accompanied by low oxygen supply due to sluggish circulation and weak vertical mixing (Oschlies et al., 2018).

80 The impact of climate change on oxygen change in coastal and shelf environments is at present not fully understood as it results from the interplay of multiple, often antagonistic, physical and ecosystem processes that render ecosystem response highly uncertain and spatially heterogeneous. Due to their limited depth, shelf seas are projected to warm up more than the open ocean (Kwiatkowski et al., 2020). In addition, the coastal and shelf ecosystems are under stronger influence from terrestrial nutrient and organic matter inputs, which can foster both primary production and respiration, while limited depth 85 and tidal mixing favour mixing-induced oxygenation. Furthermore, the diagnosis of observed and predicted oxygen dynamics may depend on the spatial scales and domains being analysed: while Gilbert et al. (2010) found recent past median oxygen decline rates to be more severe in coastal waters (defined as a 30 km band near the coast) than in the open ocean (>100 km from the coast), Kwiatkowski et al. (2020) found benthic oxygen depletion not to be predominantly confined to shelf waters in a multi-model comparison. These two findings are not necessarily inconsistent as the definition of coastal 90 waters, from Gilbert et al. (2010), differs from that of shelf waters from Kwiatkowski et al. (2020). It is also important to



note that the CMIP5 and CMIP6 earth system models used in the latter study are generally of coarse resolution (around 1 degree) and do not correctly resolve most coastal and shelf processes, or coastlines and bathymetry.

The North Western European continental shelf (NWES, Fig. 1) is located in the north-east Atlantic; it has an open connection with the Atlantic at its northern and western boundaries, along the continental slope, and with the Baltic Sea through the Danish strait. A current runs northward along much of the continental slope and is responsible for exchange with the open ocean. Oceanic waters enter the North Sea north via the Fair Isle, East Shetland and Western Norwegian Trench currents and south via the English Channel; circulation in the North Sea is counter-clockwise with water exiting along the Norwegian Trench after having joined with Baltic Sea outflow. A detailed description of the North Sea physical oceanography can be found in Huthnance (1991) and Ricker and Stanev (2020). Much of the NWES stratifies seasonally, during the boreal summer, but relatively shallow coastal areas in the southern North Sea, Irish Sea and Western English Channel that are under strong influence from tides remain well mixed throughout the year. Here mixing maintains well oxygenated bottom waters year-round, while the Central and Southern North Sea, Celtic Sea, Armorican shelf and Eastern English Channel are known to be prone to near-bed oxygen depletion (Breitburg et al., 2018; Ciavatta et al., 2016).

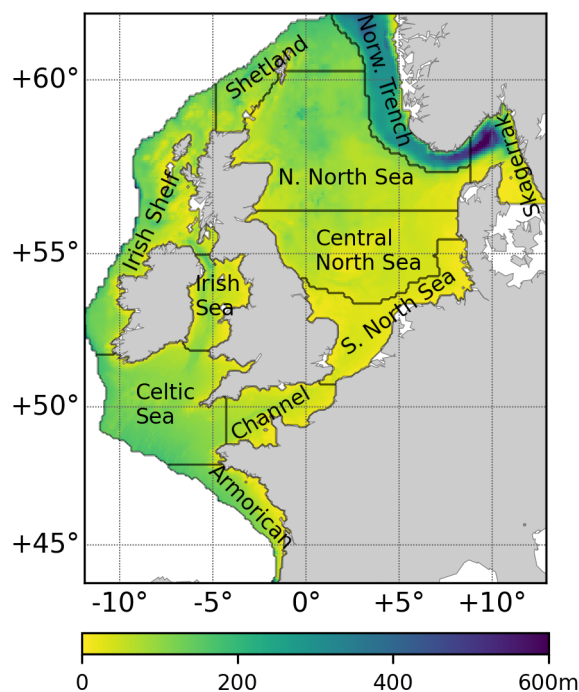


Fig. 1. The North Western European Shelf and its sub-basins considered in this study. Colour scale represents bathymetry.

When trying to assess the future evolution of oxygen in coastal and shelf ecosystems, given the uncertainty and spatio-temporal heterogeneity that characterizes deoxygenation projections, coupled physics-biogechemistry regional models are a



110 more appropriate tool compared to global models. The finer resolution of a bespoke regional model allows in fact for a better representation of small to medium scale processes than would be possible with a coarser global model (Drenkard et al., 2021; Giorgi, 2019; Holt et al., 2016).

115 For the NWES Wakelin et al. (2020) produced the first investigation on the potential change in near-bed oxygen during the 21st century under high greenhouse gas emissions (RCP8.5). The study aimed at assessing not just the projected change in near-bed oxygen levels, but also at attributing such changes to driving physical and biogeochemical processes. The authors found that while warming and freshening are generally coherent throughout the shelf, oxygen change displays pronounced spatial heterogeneity within sub-regions. The areas experiencing strong oxygen depletion become larger in the future and low oxygen periods last longer. This is due to the combined effect of warming, changes in transport and in ecosystem processes, all components characterised by spatial heterogeneity. A large hotspot of oxygen depletion develops in the eastern North Sea during the second half of the century where the major contribution to deoxygenation is increased ecosystem respiration, whereas the warming component is dominant elsewhere. This deoxygenation hotspot develops concurrently with a change in circulation that leads to reduced exchange between the Atlantic and the North Sea along its northern boundary (Holt et al., 2018).

120 That study is based on a single model run under a single climate change scenario (RCP8.5), hence it represents just one of the possible futures for the NWES. As the authors point out, the likelihood of the results can only be assessed through an ensemble of simulations that address multiple sources of model and scenario uncertainty.

125 Here we build on that work by addressing one such sources of uncertainty: intra-scenario variability. In fact, even within the same emission scenario, climate change projections may display significant variability due to differences in internal model numerics, initial conditions and forcings other than greenhouse gas concentration (Tapiador and Levizzani, 2021). We built a small (three-members) ensemble of coupled physics-biogeochemistry regional models of the NWES all running for the 21st century under the RCP8.5 scenario. These were forced with different lateral and atmospheric boundary conditions from three different earth system models from the CMIP5 collection (Taylor et al., 2012) that were chosen as they display a wide array of responses within the same emission scenario. One of our three members is the same used in Wakelin et al. (2020). Clearly a three-member ensemble is not sufficient to characterise all possible sources of uncertainty, nor to provide a robust assessment of the expected range of values. Instead, here we aim at investigating possible ecosystems responses under a sufficiently large range of expected changes, while assessing how ecosystem processes change under different conditions, and whether there are processes common to all projections.

2 Materials and methods

2.1 Ensemble description

140 All model simulations use the NEMO-ERSEM model suite and cover the 1980-2099 period under the RCP8.5 emission scenario, with a 10-year spin-up period (1980-1989) that was excluded from the present analysis. NEMO (Nucleus for



European Modelling of the Ocean, Madec et al., 2019) is an ocean general circulation model and ERSEM (European Regional Seas Ecosystem Model, Butenschön et al., 2016) is a lower trophic network model that explicitly resolves the cycles of nutrients (N, P, Si), organic and inorganic carbon and oxygen in a coupled pelagic-benthic ecosystem. While two of the three members differ in boundary and initial conditions only, the third one, being an older simulation, also employs different NEMO-ERSEM code and vertical grid, it is hence not perfectly comparable to the other two. Commonalities and differences are detailed in the following.

Atmospheric and lateral boundary conditions were derived (in different ways, details below) from three Earth System Models (ESMs) from the CMIP5 collection (Taylor et al., 2012). The parent ESMs are GFDL-ESM2G (Dunne et al., 2012), IPSL-CM5A-MR (Dufresne et al., 2013) and HADGEM2-ES (Jones et al., 2011) and were chosen as they represent a gradient of climate sensitivities, with GFDL-ESM2G showing the lowest sensitivity and HADGEM2-ES the highest (Andrews et al., 2012). The three ensemble members will be hereafter referred to as GFDL, IPSL and HADGEM for brevity. GFDL's and IPSL's boundary conditions were directly extracted from the parent ESM and interpolated onto the regional grid, while HADGEM uses as oceanic boundaries the output of a global coupled physics-biogeochemistry model (NEMO-MEDUSA, Yool et al., 2015) forced with atmospheric boundaries from the same HADGEM2-ES CMIP5 run.

All models have the same horizontal resolution of $1/15^\circ$ latitude by $1/9^\circ$ longitude (~ 7 km) while the vertical resolution differs in HADGEM (33 vertical levels, s-coordinates, i.e. terrain-following) from the other two (51 vertical levels, s-coordinates). The NEMO version also differs in HADGEM (NEMO V3.2, O'Dea et al., 2012) from the other two members (NEMO V3.6, O'Dea et al., 2017); finally, the parameterization of ERSEM functional types is different in HADGEM (Blackford et al., 2004) with respect to the other two members (Butenschon et al., 2016). The reason for these differences lies in the fact that the HADGEM model represent an older run and was in fact used in previous studies (Holt et al., 2018; Wakelin et al., 2020), while IPSL and GFDL were run more recently and are also part of a wider physics-only ensemble (see Holt et al 2022).

In IPSL and GFDL, physics initial conditions are from the parent ESM while biogeochemical variables are from a reanalysis product (Ciavatta et al., 2018), interpolated onto the regional grid. The models are forced with atmospheric temperature, pressure, wind velocity, solar radiation, humidity and precipitation from the parent ESM. Atmospheric Nitrogen deposition is common to the two members and comes from the EMEP project (<http://www.emep.int>). River discharge is from observed mean annual cycles for 250 rivers at daily frequency (Vörösmarty et al., 2000, Young and Holt, 2007), modulated by the fractional change (compared to 1984-2004 mean) in annual ESM precipitation aggregated over four land regions (1. UK and Ireland; 2. Sweden and Norway; and Continental Europe: 3. east of 2.5° E and 4. west of 2.5° E). River nutrient loads are derived from the concentrations used in Ciavatta et al. (2018) multiplied by the discharge. Atmospheric CO_2 partial pressure (Riahi et al., 2007) is also common to the two members. To determine light availability for phytoplankton we forced the models with a climatological light attenuation coefficient field derived from CMEMS ocean colour products (level 3 product 009_086, marine.copernicus.eu).



175 IPSL's and GFDL's lateral boundary conditions (open ocean and Baltic) were extracted from the parent ESMs and include all physics and biogeochemistry variables; where biogeochemical variables were not present in the parent ESM (e.g. plankton functional types) they were set to low values.

Finally, tidal forcing is as described in O'Dea et al. 2012 and O'Dea et al. 2017.

180 The HADGEM setup is similar, differing only in initial conditions (physics are from the NEMO-MEDUSA simulation that provides boundary conditions whilst biogeochemical variables are from a previous spun-up simulation), the version of EMEP nitrogen deposition (downloaded 2011), the source of the light attenuation coefficient (Smyth et al., 2006) and the treatment of the Baltic boundary (freshwater inflows). HADGEM uses the same river forcing as IPSL and GFDL but without modulation by the ESM precipitation. Full details of the HADGEM setup are given by Holt et al., (2018) and Wakelin et al., (2020).

2.2 Validation

185 Here we focus validation to the model variables that were considered in our analysis. Some validation of the HADGEM model has already been carried out in Wakelin et al. (2020). A thorough validation of the NEMO-ERSEM operational ecosystem model for the NWES can be found in Edwards et al. (2012) and in the Copernicus Quality User Information Document (Kay et al., 2020). Since climate models do not necessarily reproduce the climate system's phase, a direct point-to-point comparison with observations is not appropriate, conversely, a comparison between the model-based climatology and one based on observations is a more appropriate validation practice (Sellar et al., 2020; Yool et al., 2021). Therefore, 190 model results are assessed against the North Sea Biogeochemical Climatology (NSBC) dataset (Hinrichs et al., 2017). This dataset covers the region 47° - 65 °N and 15 °W - 15 °E (roughly the NWES minus the Armorican Sea) for the period 1960-2014 and consists of a collection of observational data for multiple physical and biogeochemical variables. Data are quality controlled and come in the form of 3D-fields of optimally interpolated parameter values.

195 For the comparison we considered the output of our models for the period 1990-2005 as 2005 is the last year of historical simulation within the CMIP5 models. As validation metrics we considered normalised bias, nbias, and normalised unbiased root mean squared distance, nurmsd (Jolliff et al., 2009); these metrics were computed for each sub-basin of the NWES (Fig. 1). Normalisation (bias and rmsd metrics are divided by the standard deviation, std, of the observations) of metrics is aimed at facilitating the comparison across models and variables.

200 2.3 Analysis of oxygen change

Oxygen change can be partitioned into different components: the first one is related to warming that negatively affects oxygen saturation concentration, hence lowering the amount of gas that can be effectively dissolved in seawater; another component is related to changes in biological processes that either consume or produce oxygen (respiration and primary production), and finally one component is related to change in transport processes responsible for oxygen supply (e.g. 205 enhanced stratification limiting atmospheric oxygen uptake and changes in circulation modifying lateral transport).



210 Wakelin et al. (2020) proposed a procedure to separate the component of oxygen change that is due to change in saturation concentration from the component linked to all other processes; this procedure is based on the assumption that oxygen concentration would equal saturation concentration were it not for processes like oxygen production, respiration and transport (or lack thereof). Considering an oxygen timeseries at a point in space, by assuming that oxygen saturation state (i.e. the ratio between in-situ concentration and concentration at saturation) does not change with time and equals SS_{t_0} , we can estimate what the oxygen concentration at time t would be, considering changes in saturation concentration alone (here named physico-chemical, phy-ch):

$$O_{2,phy-ch,t} = SS_{t_0} \cdot O_{2,sat,t} \quad (1)$$

215

Where $O_{2,sat,t}$ is the oxygen saturation concentration at time t . We can then single out the component of change due to change in concentration at saturation:

$$\Delta O_{2,phy-ch} = O_{2,phy-ch,t} - O_{2,t_0} = SS_{t_0} \cdot (O_{2,sat,t} - O_{2,sat,t_0}) \quad (2)$$

220

where O_{2,t_0} and O_{2,sat,t_0} are oxygen concentration and saturation concentration at the beginning of the timeseries. The difference between $O_{2,phy-ch,t}$ and oxygen at time t , $O_{2,t}$, gives the portion of change ascribable to all other processes:

$$\Delta O_{2,other} = O_{2,t} - O_{2,phy-ch,t} = O_{2,sat,t} \cdot (SS_t - SS_{t_0}) \quad (3)$$

225

It can be observed that, by definition the sign of the $\Delta O_{2,phy-ch}$ component is controlled by $O_{2,sat,t}$ (eq. 2) and the sign of $\Delta O_{2,other}$ by SS_t (eq. 3), hence these two variables will explain much of the variability of the all the ΔO_2 metrics. Here values at time t are monthly average values and values at time t_0 are monthly climatologies over the first 30 years of simulation.

230 To assess change we studied the spatial distribution of biogeochemical variables' change in the three models by comparing the average values of the first and last 30 years of simulation (1990-2019 and 2070-2099). By comparing 30 year windows at the two ends of the simulation period, we remove any potential impact of short-term inter-annual variability in our analysis. To assess relationships between variables, we computed point-to-point correlations (spearman correlation with significance threshold $p < 0.01$) using monthly averaged data; linear trend and average seasonal (monthly) cycle were removed from the time-series prior to the calculation of correlation coefficients to minimise type I errors (i.e. false positives) when the seasonal cycle and/or long term trend dominate the correlation (Legendre and Legendre, 2012).

235

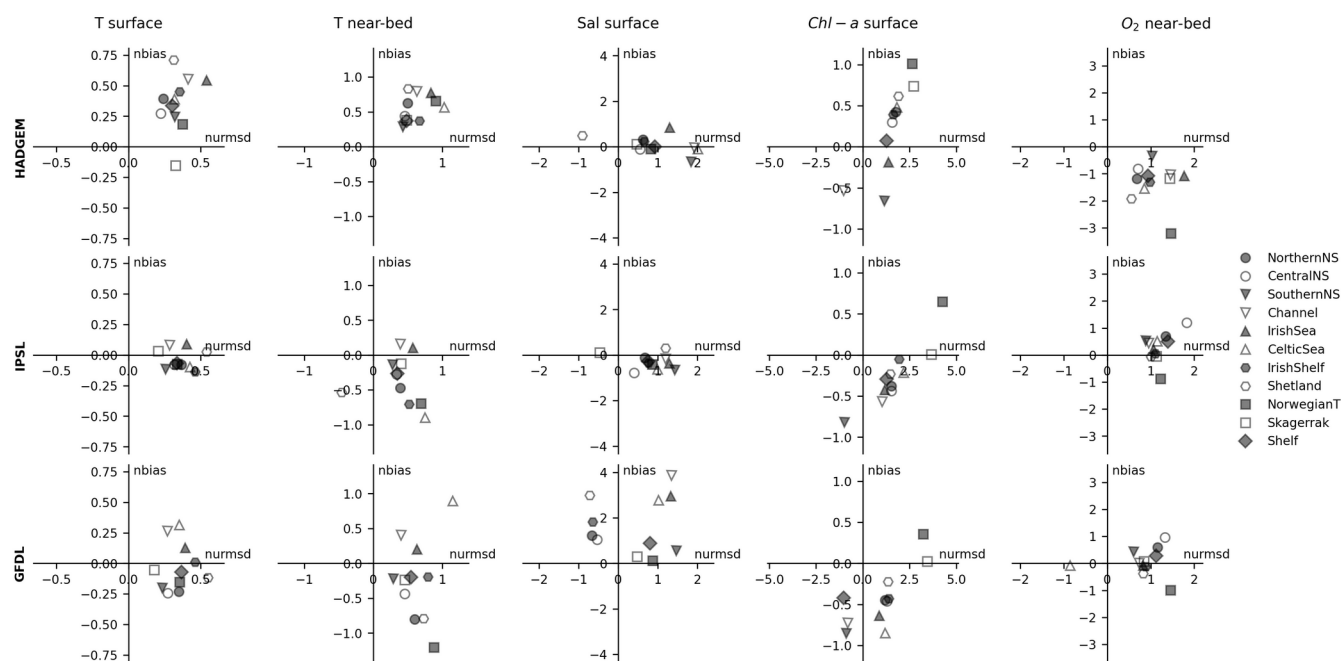
We decided to compute correlations between $O_{2,sat,t}$, SS_t (instead of $\Delta O_{2,phy-ch}$, $\Delta O_{2,other}$) and other variables because, due to the definitions in eq. 2 and 3, correlations would not change.



3 Results

3.1 Models' validation

240 Validation results are shown in Fig. 2. The comparison of both surface and near bed temperature with NSBC climatological data reveals a considerable positive bias of HADGEM (up to 0.75 stds) and higher nurmsd than the other two models. IPSL and GFDL perform better, with nurmsd generally within 0.5 stds and nbias generally within 0.25 for surface values but greater for bottom values. Of the two models IPSL shows the best performance, especially for surface values. Surface salinity (here analysed because of its relation to stratification) is well represented in both the HADGEM and IPSL models, with nbias, nurmsd values generally within 0.5 std, whilst the GFDL model displays a considerable positive bias, with values between three and four stds in the Channel, Irish Sea, Shetland and Celtic Sea. Surface chlorophyll-a (here considered as a proxy for primary production) is fairly well represented in all models, with nbias values always within one std; on average HADGEM displays a positive bias in representing surface chlorophyll, while IPSL and GFDL a negative one, although this is not consistent across all subdomains. nurmsd values range approximately between one and five stds, but normally within 2.5 stds, and comparable across models. As for near bed oxygen, the HADGEM model shows a negative bias against NSBC data and nurmsd values of 0.5 to two stds. IPSL and GFDL perform better, overall they display a slightly positive bias, generally within one std. Finally, nurmsd values are generally positive, meaning that the std of the models is almost always larger than that of the NSBC dataset.





255 **Fig. 2.** Validation results. Plots show nbias vs nurmsd for selected variables in the three ensemble models and in different model subdomains.

3.2 Changes in temperature and salinity

260 All three models consistently predict warming and freshening of the NWES (Fig. 3). The climate sensitivity ranking of the three parent ESMs (Andrews et al., 2012) is reflected in the downscaled projections, with HADGEM showing the highest warming and freshening, GFDL the lowest and IPSL in between. The projected surface warming is mostly uniform throughout the NWES, with slightly more intense warming in shallower areas, whereas freshening is more intense along the Skagerrak/ Norwegian Trench (also in GFDL where freshening is however very low) and in the Eastern North Sea.

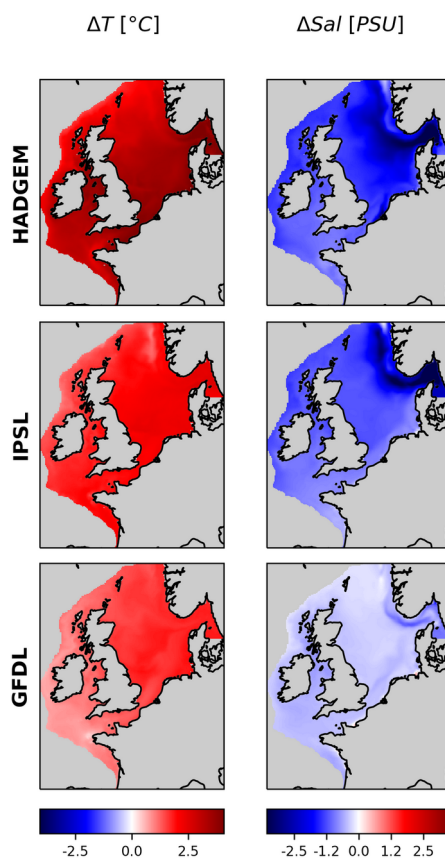


Fig. 3. Surface temperature and salinity, difference between future (2070-2099) and present (1990-2019) periods.



265 3.3 Near-bed oxygen current state and change

270 All three ensemble members consistently show a decrease in near-bed oxygen throughout the shelf (Fig. 4). The severity of the impacts follows the three models' climate sensitivity: GFDL shows the least change ($\sim 0.3 \text{ mg L}^{-1}$ averaged over the shelf), and no relevant hotspots of oxygen decline are present; IPSL shows localized hotspots of intense oxygen decline along the Skagerrak and Norwegian Trench and along the western shelf margin ($\sim 1 \text{ mg L}^{-1}$ for Skagerrak and Norwegian trench combined) but less severe impacts, similarly to GFDL, on the rest of the shelf; HADGEM shows the severest impacts, with all the eastern North Sea showing declines of $> 1 \text{ mg L}^{-1}$ while also in the rest of the domain near-bed oxygen declines more than in the other two models.

275 Intense change in HADGEM results in widespread exceedance of hypoxia thresholds (Fig. 4, defined as average monthly concentration $< 6 \text{ mg L}^{-1}$ (OSPAR, 2003)) in the North Sea under future conditions; this feature is still present but less prominent in IPSL and even less so in GFDL. Note that to calculate hypoxia thresholds exceedances, due to different biases in the models (Fig. 2), model runs were bias-corrected, i.e. point-to-point model values were adjusted so that their temporal mean in the reference period equals that of the NSBC database.

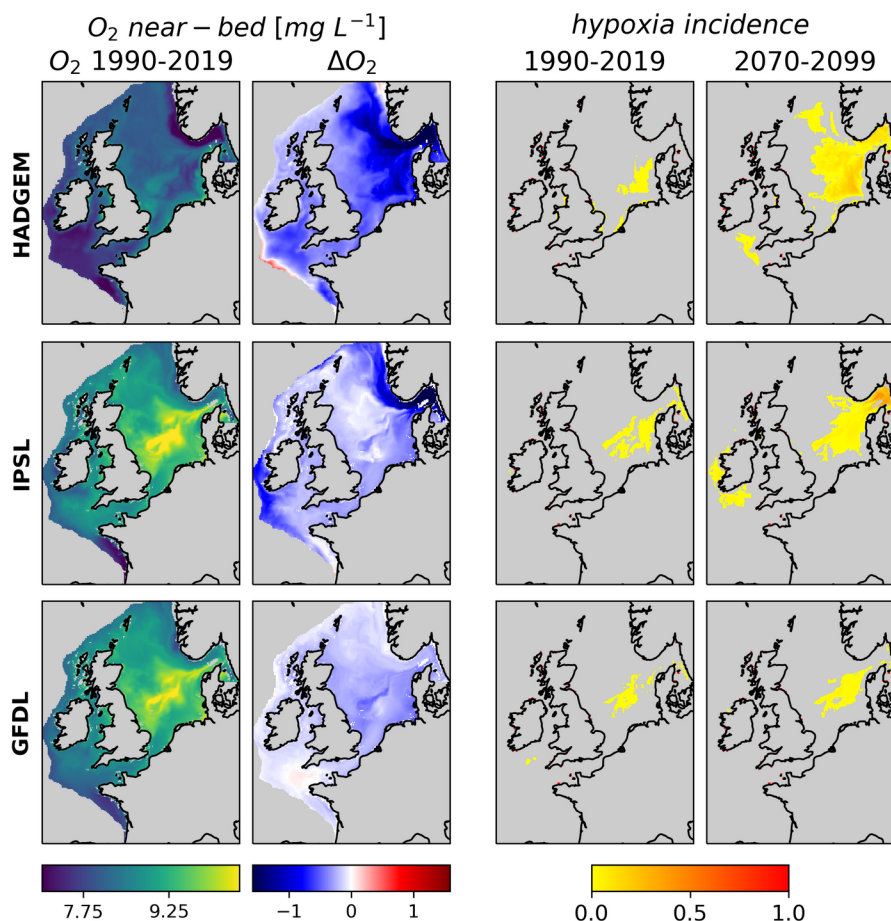


Fig. 4. Near-bed O₂ concentration, present state (average of 1990-2019) and change (difference of the 2070-2099 and 1990-2019 averages) And fraction of year with average near-bed Oxygen < 6 mg L⁻¹ under present day and future conditions, calculated on bias-corrected data.

3.4 Contributions to near-bed oxygen change

Figure 5 shows how the components of oxygen change ($\Delta O_{2,phy-ch}$ and $\Delta O_{2,other}$) contribute to determine the final change projected by the models. $\Delta O_{2,phy-ch}$ is fairly uniform throughout the shelf and its intensity follows the climate sensitivity of the driving ESM. $\Delta O_{2,other}$ instead shows significant variability both across models and, spatially, within models, with large areas even showing an increase. In GFDL $\Delta O_{2,other}$ accounts for $\sim +0.2$ mg L⁻¹ throughout the shelf, partially counterbalancing $\Delta O_{2,phy-ch}$ (~ -0.3 mg L⁻¹); in IPSL $\Delta O_{2,other}$ is strongly negative in the Norwegian Trench and Skagerrak and, to a lesser extent, along the western shelf margin (~ -0.5 mg L⁻¹ in the trench, ~ -2.0 mg L⁻¹ in the Skagerrak), thus explaining the hotspots of oxygen decline in these areas, while $\Delta O_{2,other}$ is positive in the North Sea ($\sim +0.2$ mg L⁻¹), partially counterbalancing $\Delta O_{2,phy-ch}$;



290 in HADGEM the vast hotspot of declining near-bed oxygen encompassing the eastern North Sea, Norwegian Trench and Skagerrak is explained by the combined effect of $\Delta O_{2,phy-ch}$ and $\Delta O_{2,other}$, with the latter accounting for the largest share of the decline (up to $\sim -1.0 \text{ mg L}^{-1}$ in the trench, $\sim -1.5 \text{ mg L}^{-1}$ in the Skagerrak), while in the western North Sea, English Channel, Irish Sea and western shelf margin $\Delta O_{2,other}$ is positive. Fig. 5 also shows how $\Delta O_{2,sat}$ closely traces $\Delta O_{2,phy-ch}$ and ΔSS_{O_2} closely traces $\Delta O_{2,other}$, as expected from eq. 2 and 3.

295 In the following sections, the drivers behind this different patterns will be analysed.

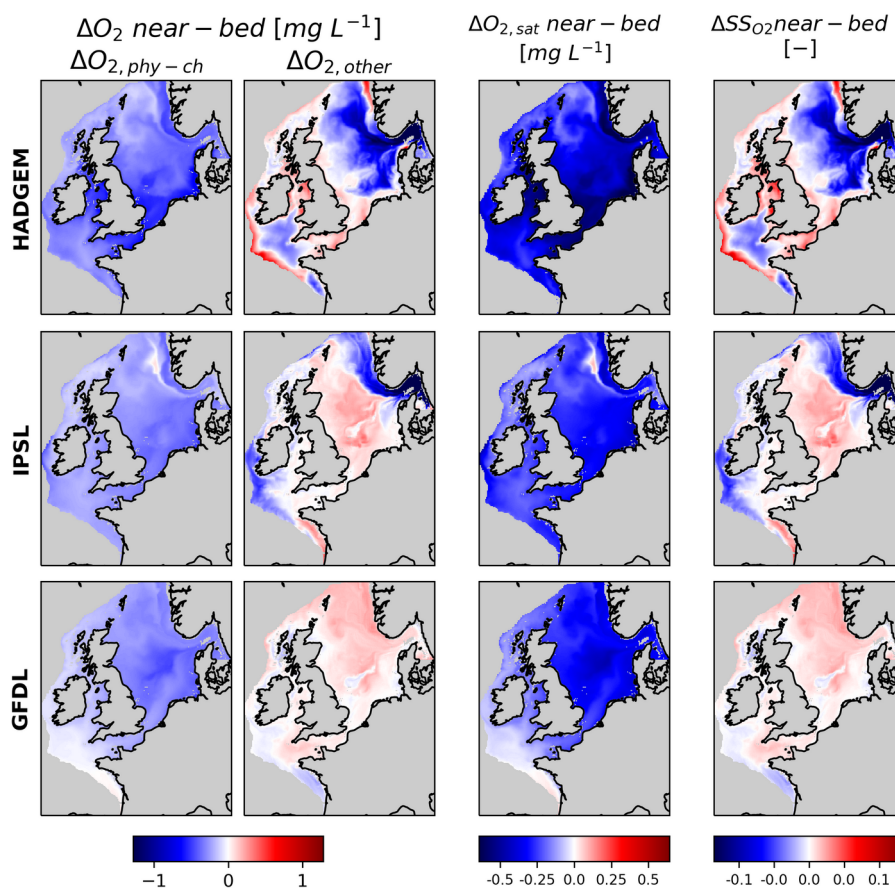


Fig. 5. contributions of near-bed oxygen change, $\Delta O_{2,phy-ch}$ and $\Delta O_{2,other}$, change in O_2 saturation state and O_2 saturation concentration. Note that the spatial distribution of $\Delta O_{2,sat}$ and ΔSS_{O_2} closely follows that of $\Delta O_{2,phy-ch}$ and $\Delta O_{2,other}$ respectively.

3.5 Controls of near-bed oxygen change components: Temperature

300 Changes in $\Delta O_{2,phy-ch}$ and $O_{2,sat}$ are, for the greatest part, explained by warming (correlation between $O_{2,sat}$ and near-bed T ~ -1 everywhere in all models, not shown). The driver of this is the temperature atmospheric forcing (Fig. 6) that in all models displays strong negative correlation with near-bed $O_{2,sat}$, especially in the shallow and well-mixed southern North Sea and



Channel, while the correlation is weaker along the deeper Norwegian Trench. Conversely atmospheric temperature correlates positively with SS_{O_2} in coastal regions only (including the Southern North Sea and Channel) and is not significant in the Eastern North Sea and along the Norwegian Trench. This suggests that other processes are driving the decline in SS_{O_2} that leads to the deoxygenation hotspots in these areas.

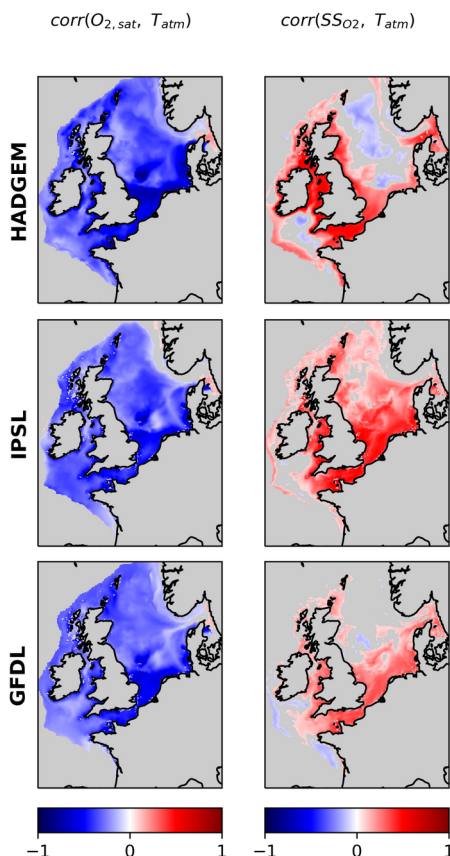


Fig. 6. correlation between Temperature atmospheric forcing and near-bed $O_{2,sat}$ and SS_{O_2} .

3.6 Controls of near-bed oxygen change components: Stratification

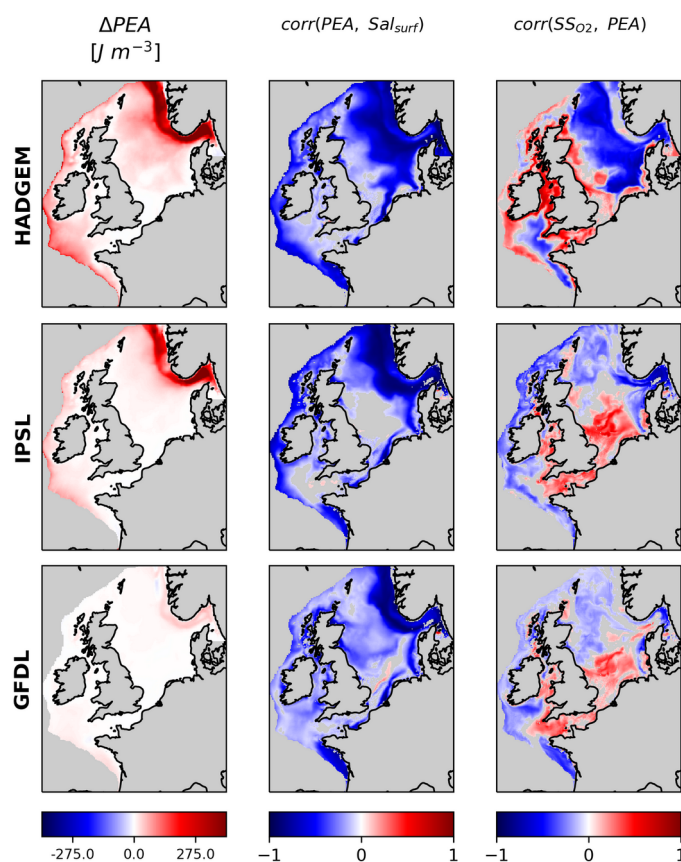
The Eastern North Sea hotspot of oxygen decline in HADGEM coincides with an enhanced stratification hotspot and in fact SS_{O_2} and potential energy anomaly (PEA - an indicator of stratification de Boer et al. 2008) are strongly negatively correlated in this area (Fig. 7); the same is true for the Skagerrak in both HADGEM and IPSL, but curiously SS_{O_2} along the Norwegian trench seems to be only in part correlated with PEA in both IPSL and HADGEM).

This lack of correlation is due to different phenomena: the first one is the strong advective nature of the Norwegian trench system that spatially decouples causes from effects, rendering point-to-point correlation not suitable in this area; correlations



do in fact become significant when the average values over the Norwegian trench are considered (Fig. 8). Even so, in HADGEM only, there also is a progressive change in the sign of the correlation, from negative to positive, starting about 2050 to the end of the simulation, that renders the correlation for the whole timeseries non-significant. Conversely a significant negative correlation is obtained by discarding the data from 2060 on.

320 GFDL on the other hand only shows a moderate increase in stratification and no significant hotspots, with a weaker correlation between SS_{O_2} and PEA than in the other two models. The main driver of stratification along the Norwegian Trench and in the Eastern North Sea, for all models, is surface salinity, that in fact is strongly negatively correlated with PEA there.



325 **Fig. 7.** Change in potential energy anomaly (PEA) and correlation between PEA and surface salinity and PEA and SS_{O_2} .

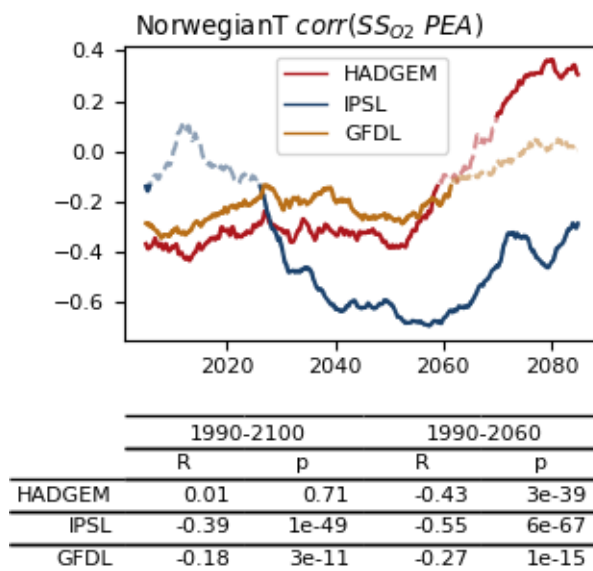


Fig. 8. mean Norwegian trench values, running correlations (30-year window) between SS_{O2} and PEA for the three simulations (line plots, dashed lines have $p > 0.01$) and correlations for the 1990-2100 and 1990-2060 periods.

330 3.7 Controls of near-bed oxygen change components: Primary Production

In all models, and especially in IPSL and GFDL, depth integrated net primary production (NPP) decreases in the North Sea and along the shelf edge due to decreasing oceanic nutrient input (fig 9), similarly to what was shown by Holt et al. (2012, 2016). In the shallow and well mixed southern North Sea, English Channel and Irish Sea, on the contrary, NPP increases providing additional oxygenation, as shown by the positive correlation between SS_{O2} and NPP (fig 9).

335 On the contrary, in HADGEM, NPP is negatively correlated with SS_{O2} in the deeper and seasonally stratified eastern North Sea, Skagerrak and Norwegian Trench; here NPP contributes to oxygen decline by providing increased organic matter that sinks and is later respired. The same effect is present also in the IPSL model, but limited to the Skagerrak.

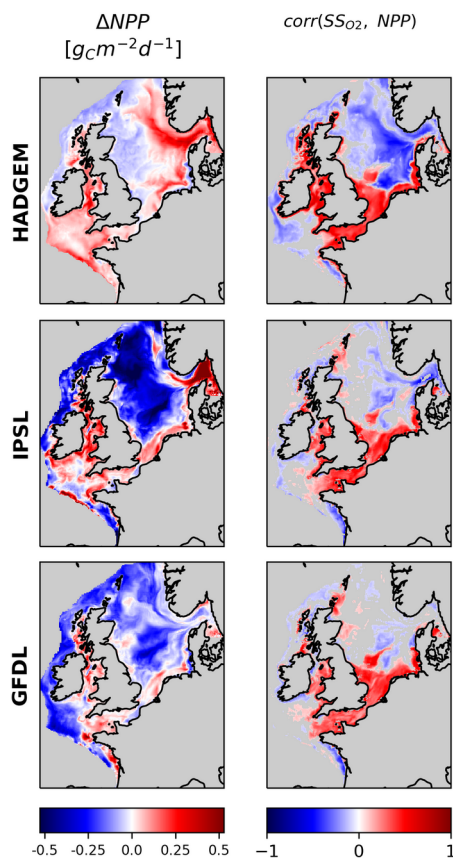


Fig. 9. Change in depth integrated net primary production (NPP) and correlation between NPP and SS_{O_2} .

340 3.8 Controls of near-bed oxygen change components: Bacterial Respiration

Bacterial respiration is the largest contribution of total community respiration, given their faster turnover, hence here we will focus only on this component. Furthermore, the result of the analysis does not change significantly when community respiration is considered (not shown).

In HADGEM near-bed bacterial respiration (BResp, Fig. 10) significantly increases in the eastern North Sea, fuelled by
345 increasing NPP and warming, thus contributing, in tandem with enhanced stratification, to oxygen decline; SS_{O_2} and BResp are in fact significantly negatively correlated in this area.

BResp instead decreases throughout most of the North Sea and along the shelf margin in IPSL and GFDL, suggesting reduced oxygen consumption as a possible mechanism for the observed increase in SS_{O_2} . However, when all monthly values are considered, the correlation between SS_{O_2} and BResp is rather weak and positive (instead of negative as would be
350 expected), especially in the central North Sea, for both models. This is because simple point-to-point correlation over the



355 full period, does not allow to capture seasonally heterogeneous processes; in fact, a significant negative correlation between SS_{O_2} and BResp is detected for the central and northern North Sea in both IPSL and GFDL when singling out the months from November to March. This is because during winter months, with little primary production, respiration is a dominant contribution to oxygen levels. Instead, during the remainder of the year (growth season), the correlation is weakly positive or non-significant (not shown).

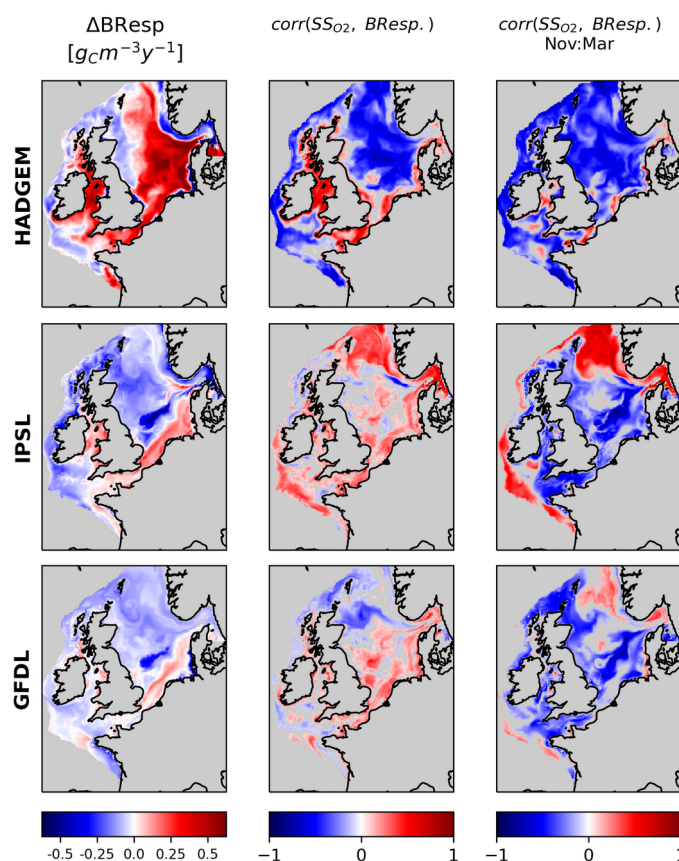


Fig. 10. Change in near-bed bacterial respiration and correlation between BResp and SS_{O_2} for all months and for months from November to March alone.

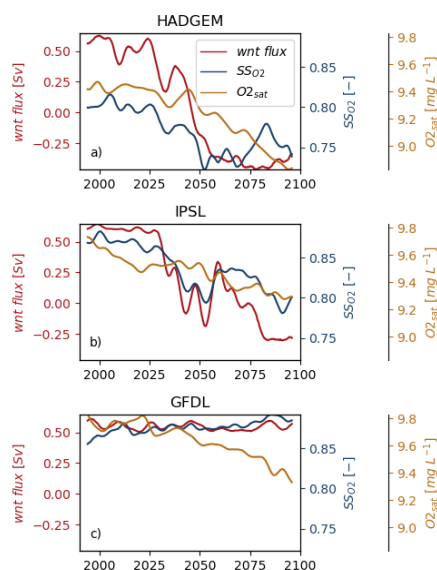
360 3.9 Impact of abrupt changes in circulation on the emergence of de-oxygenation hotspots

The onset of the development of deoxygenation hotspots in the eastern North Sea, Skagerrak and Norwegian Trench in HADGEM and IPSL is tied to a progressive weakening and reversal of the western Norwegian Trench Current (wnt, Fig. 11a,b) starting approximately in the mid 2020s for both models (Holt et al., 2018). The time evolution of SS_{O_2} in this area is



in fact tightly coupled with that of the western Norwegian Trench current in both members. This circulation change is absent
 365 from GFDL (Fig. 11c) that in fact also lacks significant deoxygenation hotspots.

This suggests that the circulation change, by driving the observed freshening and increase in stratification in the North Sea, is the main driver of the development of deoxygenation hotspots. The time evolution of $O_{2,sat}$ also appears coupled with current flux but to a lesser extent, especially in IPSL where $O_{2,sat}$ starts declining well before the onset of circulation changes.



370 **Fig. 11.** Temporal evolution of SSO_2 and $O_{2,sat}$ in the Norwegian Trench and Western Norwegian Trench current flux; monthly average data are smoothed with a Gaussian filter. Positive values of the current are entering the North Sea.

4 Discussion

We studied the spatio-temporal evolution of near-bed oxygen concentration in the NWES in a three-member ensemble of coupled physics-biogeochemistry models running from 1980 to 2100 under a high emissions scenario (RCP8.5). Building on
 375 previous work on oxygen (Wakelin et al., 2020) and circulation (Holt et al., 2018) changes in the NWES, we added an intra-scenario variability dimension by using three instances of the same model suite (albeit with one member differing in model version and parameterisation) forced with boundary conditions from three global models covering a wide spectrum of climate sensitivities. This allowed to verify whether the models' response, and the processes involved, show any commonalities and/or differences, and how ecosystem response is related to the projected intensity of climate change.

380 All ensemble members consistently predicted a decline in near-bed oxygen throughout the shelf. Our results confirm those of Wakelin et al. (2020), that, whilst responses of the physical system (warming, freshening) are generally homogeneous throughout the shelf, near-bed oxygen change can display marked spatial heterogeneity with hotspots of change as well as



areas where antagonistic processes mitigate ecosystem response. However, by using an ensemble of simulations we show that these hotspots of change occur only in the members with the highest climate sensitivity (HADGEM and IPSL), whilst
385 for relatively low levels of climate change (GFDL) the ecosystem response is largely homogeneous. The large areas experiencing hypoxia ($O_2 < 6 \text{ mg L}^{-1}$) identified in Wakelin et al. (2020) only emerge when the strongest change in climate is projected by HADGEM, whilst the other two members are largely spared by critical hypoxia.

By separating the components of oxygen change into two terms related to change in $O_{2,\text{sat}}$ (largely related to warming) and SS_{O_2} (related to transport and ecosystem processes) we were able to disentangle the contributions of different processes to
390 deoxygenation. Similarly to what found in Wakelin et al. (2020) using this same approach, we show how areas of differential change are determined by combinations of transport (here atmosphere-ocean exchange, mediated by changes in stratification, rather than lateral transport) and ecosystem (increased primary production fuelling near-bed respiration) processes; on top of this, warming superimposes a spatially uniform decrease in near-bed oxygen throughout the shelf. But again, spatial heterogeneity only emerges in ensemble members with high climate change intensity, so that for low levels of climate
395 change, near-bed oxygen decline remains largely homogeneous across the NWES.

Our results also highlight the importance of increasing stratification and circulation changes in driving deoxygenation processes in coastal and shelf ecosystems. In fact, in the two most climate sensitive ensemble members, prominent hotspots of deoxygenation develop along the Skagerrak/ Norwegian trench complex and (in HADGEM only) eastern North Sea; the onset and development of these hotspots is tightly coupled with a major circulation change in the area that largely limits
400 ocean-shelf exchange processes along the northern boundary of the North Sea. This circulation change has already been identified by Holt et al. (2018) by using the same model run as our HADGEM member; according to the authors, this decrease in western Norwegian Trench inflow can be traced to a substantial increase in stratification at the entrance to the Trench, limiting the ability of the slope current to steer into the North Sea. Reduced exchange with the open ocean contributes to a freshening of the Norwegian Trench and Eastern North Sea, that fill up with Baltic and river waters, driving
405 the increase in stratification. Moreover, the results here are consistent with the observation by Tinker et al. (2016) that the large circulation changes occur only in their downscaled ensemble members with highest climate sensitivity in the driving climate model (3 out of 11 members in that case).

As mentioned earlier, HADGEM uses a different NEMO-ERSEM configuration than the other two members. This does not seem to have first order consequences for ocean physics, as the response of the three models in terms of changes in
410 temperature, salinity and stratification appears largely coherent with the progressive levels of climate sensitivity represented. Also the biogeochemical response in the Southern North Sea, English Channel and Irish Sea is largely comparable across models. However, in the Eastern North Sea and Norwegian Trench areas HADGEM does display a noticeably different response when it comes to changes in primary production and respiration and in the correlation between these variables and near-bed oxygen. In particular the link between net primary production, respiration and near-bed oxygen appears much
415 tighter in HADGEM, as testified by stronger correlations. This is likely a consequence of the change in the parameter set of



the biogeochemical model for both phytoplankton and bacteria in the recent update (Butenschön et al., 2016) compared to the original one (Blackford et al., 2004).

The method we used to disentangle the contributions of different physical and ecosystem processes to deoxygenation has allowed to understand the interactions among the processes driving changes in oxygen. We attributed the changes in $O_{2,sat}$ to warming while changes in SS_{O_2} are related to transport and ecosystem processes.

Here we mostly analysed model output by mapping point-to-point correlation between variables and, whilst this approach has proven useful in highlighting potential cause and effect mechanisms, it also has limits. In fact such an approach is prone to failure in identifying significant correlations when transport makes causes and effects spatially decoupled, for example in highly advective systems such as the Norwegian Trench, and/or when the relations between system variables change in time, either seasonally or on multiannual timescales. Future studies should take these limitations into account, for example by applying this analysis jointly with an assessment of flux budgets and/or averaging over regions and periods with homogeneous characteristics, to address spatial decoupling of processes, and/or by studying how the relations between system variables change in time.

5 Conclusions

Our results about the contributions of different components of oxygen change highlight the importance of using detailed biogeochemical models, such as ERSEM, while evaluating oxygen change. In fact, it is well known that current climate models tend to underestimate recent rates of oxygen decline (Oschlies et al., 2018, 2017), however some authors pointed out how modelled solubility-driven changes largely agree with observations, hinting at model deficiencies in representing biogeochemical cycles and changes in circulation and mixing processes (Oschlies et al., 2018). This is especially true for coastal and shelf ecosystems such as the NWES, where small scale processes are poorly represented in global models, and the interplay of multiple physical and biogeochemical processes is especially complex and spatially heterogeneous. Furthermore, current global climate models differ widely in the complexity with which they represent biogeochemical cycles, with some of them adopting fairly simple approaches (Kearney et al., 2021). In fact, while current global models on average project a decline in subsurface oxygen, there still is a high degree of variability in projections at regional scales (Kwiatkowski et al., 2020).

This study also serves to highlight the suitability of regional models for the study of coastal and shelf processes that are not adequately represented in global models. The drawback is that not enough regional simulations are yet available to construct robust climate change assessments as is possible with global models. Here we in fact used a limited number of realizations (three) of the same coupled model suite and only one climate change scenario, and albeit we did explore intra-scenario variability to some degree, this can by no means considered a robust assessment of expected change.



We suggest that future efforts should be directed at collating ensembles of regional climate model projections (similarly to what done within the World Climate Model Intercomparison Project, CMIP), for the purpose of studying marine climate and ecosystem impacts and controls, including those on oxygen.

450 When assessing the potential impacts of climate change on marine species, near-bed oxygen concentration is a particularly significant variable because it dictates habitat viability for benthic sessile and scarcely motile species that cannot move quickly to more favourable conditions.

455 Exposure to oxygen levels below critical values do result in mortality, but also sub-lethal effects from reduced oxygen are of concern. Oxygen supply, which is modulated by temperature, has been proposed as a factor explaining maximal attainable size (Verberk et al., 2021) and geographic distribution (Deutsch et al., 2015) in marine species. Future deoxygenation, combined with warming, has hence the potential to alter marine ecosystems even where critical low oxygen concentrations are not exceeded. Our results consistently point at decreasing near-bed oxygen levels in the NWES during the next century, a change that will inevitably reflect on the viability and ecological function of benthic ecosystems.

460 **Code availability.** NEMO and ERSEM are both free and open source, their code can be retrieved from the PML github repository (github.com/pmlmodelling). NEMO was used in a configuration called AMM7 that models the NWES domain.

465 **Data Availability.** The physics model data for GFDL and IPSL are available here: <https://gws-access.jasmin.ac.uk/public/recicle/>, the physics model data for HADGEM are available here: <https://zenodo.org/record/3953801#.ZeusdNLMJyZ>, the biogeochemical model data for all three ensemble members are available from the corresponding author upon request. The rest of the data used in this study were published by their authors as cited in the paper.

470 **Author Contributions.** GG performed the analyses and wrote the main body of text, GG, YA and SW designed the analysis framework, all authors were involved in revising the manuscript, all authors contributed to model development and ran the simulations.

475 **Financial support.** This project has received funding from the European Union's Horizon 2020 research and innovation programme under grant agreement No 820989 (project COMFORT, Our common future ocean in the Earth system – quantifying coupled cycles of carbon, oxygen, and nutrients for determining and achieving safe operating spaces with respect to tipping points), and from the NERC projects RECICLE (Resolving climate impacts on shelf and coastal sea ecosystems NE/M004120/1 and NE/M003477/2), FOCUS (Future states of the global coastal ocean: understanding for solutions – NE/X006271/1) and CLASS (Climate Linked Atlantic Sector Science – NE/R015953/1). This work used the ARCHER and ARCHER2 UK National Supercomputing Service (<http://www.archer2.ac.uk>, last access: 26 April 2023).



480 **Competing interests.** The authors declare that they have no conflict of interest.

Disclaimer. The work reflects only the author's/authors' view; the European Commission and their executive agency are not responsible for any use that may be made of the information the work contains.

References

- 485 Andrews, T., Gregory, J. M., Webb, M. J., and Taylor, K. E.: Forcing, feedbacks and climate sensitivity in CMIP5 coupled atmosphere-ocean climate models: CLIMATE SENSITIVITY IN CMIP5 MODELS, *Geophys. Res. Lett.*, 39, n/a-n/a, <https://doi.org/10.1029/2012GL051607>, 2012.
- Bindoff, N. L., Cheung, W. W. L., Kairo, J. G., Arístegui, J., Guinder, V. A., Hallberg, R., Hilmi, N., Jiao, N., Karim, M. S., Levin, L., O'Donoghue, S., Purca Cuicapusa, S. R., Rinkevich, B., Suga, T., Tagliabue, A., and Williamson, P.: Changing
490 Ocean, Marine Ecosystems, and Dependent Communities, in: *The Ocean and Cryosphere in a Changing Climate: Special Report of the Intergovernmental Panel on Climate Change*, 1st ed., Cambridge University Press, <https://doi.org/10.1017/9781009157964>, 2019.
- Blackford, J. C., Allen, J. I., and Gilbert, F. J.: Ecosystem dynamics at six contrasting sites: a generic modelling study, *J. Mar. Syst.*, 25, 2004.
- 495 de Boer, G. J., Pietrzak, J. D., and Winterwerp, J. C.: Using the potential energy anomaly equation to investigate tidal straining and advection of stratification in a region of freshwater influence, *Ocean Model.*, 22, 1–11, <https://doi.org/10.1016/j.ocemod.2007.12.003>, 2008.
- Bopp, L., Resplandy, L., Orr, J. C., Doney, S. C., Dunne, J. P., Gehlen, M., Halloran, P., Heinze, C., Ilyina, T., Séférian, R., Tjiputra, J., and Vichi, M.: Multiple stressors of ocean ecosystems in the 21st century: projections with CMIP5 models,
500 *Biogeosciences*, 10, 6225–6245, <https://doi.org/10.5194/bg-10-6225-2013>, 2013.
- Breitburg, D., Levin, L. A., Oschlies, A., Grégoire, M., Chavez, F. P., Conley, D. J., Garçon, V., Gilbert, D., Gutiérrez, D., Isensee, K., Jacinto, G. S., Limburg, K. E., Montes, I., Naqvi, S. W. A., Pitcher, G. C., Rabalais, N. N., Roman, M. R., Rose, K. A., Seibel, B. A., Telszewski, M., Yasuhara, M., and Zhang, J.: Declining oxygen in the global ocean and coastal waters, *Science*, 359, eaam7240, <https://doi.org/10.1126/science.aam7240>, 2018.
- 505 Butenschön, M., Clark, J., Aldridge, J. N., Allen, J. I., Artioli, Y., Blackford, J., Bruggeman, J., Cazenave, P., Ciavatta, S., Kay, S., Lessin, G., van Leeuwen, S., van der Molen, J., de Mora, L., Polimene, L., Saille, S., Stephens, N., and Torres, R.: ERSEM 15.06: a generic model for marine biogeochemistry and the ecosystem dynamics of the lower trophic levels, *Geosci. Model Dev.*, 9, 1293–1339, <https://doi.org/10.5194/gmd-9-1293-2016>, 2016.
- Ciavatta, S., Kay, S., Saux-Picart, S., Butenschön, M., and Allen, J. I.: Decadal reanalysis of biogeochemical indicators and
510 fluxes in the North West European shelf-sea ecosystem, *J. Geophys. Res. Oceans*, 121, 1824–1845, <https://doi.org/10.1002/2015JC011496>, 2016.



- Ciavatta, S., Brewin, R. J. W., Skákala, J., Polimene, L., de Mora, L., Artioli, Y., and Allen, J. I.: Assimilation of Ocean-Color Plankton Functional Types to Improve Marine Ecosystem Simulations, *J. Geophys. Res. Oceans*, 123, 834–854, <https://doi.org/10.1002/2017JC013490>, 2018.
- 515 Deutsch, C., Ferrel, A., Seibel, B., Pörtner, H.-O., and Huey, R. B.: Climate change tightens a metabolic constraint on marine habitats, *Science*, 348, 1132–1135, <https://doi.org/10.1126/science.aaa1605>, 2015.
- Drenkard, E. J., Stock, C., Ross, A. C., Dixon, K. W., Adcroft, A., Alexander, M., Balaji, V., Bograd, S. J., Butenschön, M., Cheng, W., Curchitser, E., Lorenzo, E. D., Dussin, R., Haynie, A. C., Harrison, M., Hermann, A., Hollowed, A., Holsman, K., Holt, J., Jacox, M. G., Jang, C. J., Kearney, K. A., Muhling, B. A., Buil, M. P., Saba, V., Sandø, A. B., Tommasi, D., and
- 520 Wang, M.: Next-generation regional ocean projections for living marine resource management in a changing climate, *ICES J. Mar. Sci.*, 78, 1969–1987, <https://doi.org/10.1093/icesjms/fsab100>, 2021.
- Dufresne, J.-L., Foujols, M.-A., Denvil, S., Caubel, A., Marti, O., Aumont, O., Balkanski, Y., Bekki, S., Bellenger, H., Benschila, R., Bony, S., Bopp, L., Braconnot, P., Brockmann, P., Cadule, P., Cheruy, F., Codron, F., Cozic, A., Cugnet, D., de Noblet, N., Duvel, J.-P., Ethé, C., Fairhead, L., Fichet, T., Flavoni, S., Friedlingstein, P., Grandpeix, J.-Y., Guez, L.,
- 525 Guilyardi, E., Hauglustaine, D., Hourdin, F., Idelkadi, A., Ghattas, J., Joussaume, S., Kageyama, M., Krinner, G., Labetoulle, S., Lahellec, A., Lefebvre, M.-P., Lefebvre, F., Levy, C., Li, Z. X., Lloyd, J., Lott, F., Madec, G., Mancip, M., Marchand, M., Masson, S., Meurdesoif, Y., Mignot, J., Musat, I., Parouty, S., Polcher, J., Rio, C., Schulz, M., Swingedouw, D., Szopa, S., Talandier, C., Terray, P., Viovy, N., and Vuichard, N.: Climate change projections using the IPSL-CM5 Earth System Model: from CMIP3 to CMIP5, *Clim. Dyn.*, 40, 2123–2165, <https://doi.org/10.1007/s00382-012-1636-1>, 2013.
- 530 Dunne, J. P., John, J. G., Adcroft, A. J., Griffies, S. M., Hallberg, R. W., Shevliakova, E., Stouffer, R. J., Cooke, W., Dunne, K. A., Harrison, M. J., Krasting, J. P., Malyshev, S. L., Milly, P. C. D., Phillipps, P. J., Sentman, L. T., Samuels, B. L., Spelman, M. J., Winton, M., Wittenberg, A. T., and Zadeh, N.: GFDL’s ESM2 Global Coupled Climate–Carbon Earth System Models. Part I: Physical Formulation and Baseline Simulation Characteristics, *J. Clim.*, 25, 6646–6665, <https://doi.org/10.1175/JCLI-D-11-00560.1>, 2012.
- 535 Edwards, K. P., Barciela, R., and Butenschön, M.: Validation of the NEMO-ERSEM operational ecosystem model for the North West European Continental Shelf, *Ocean Sci.*, 8, 983–1000, <https://doi.org/10.5194/os-8-983-2012>, 2012.
- Gilbert, D., Rabalais, N. N., Díaz, R. J., and Zhang, J.: Evidence for greater oxygen decline rates in the coastal ocean than in the open ocean, *Biogeosciences*, 7, 2283–2296, <https://doi.org/10.5194/bg-7-2283-2010>, 2010.
- Giorgi, F.: Thirty Years of Regional Climate Modeling: Where Are We and Where Are We Going next?, *J. Geophys. Res.*
- 540 *Atmospheres*, 2018JD030094, <https://doi.org/10.1029/2018JD030094>, 2019.
- Hinrichs, I., Gouretski, V., Pätsch, J., Emeis, K.-C., and Stammer, D.: North Sea Biogeochemical Climatology (Version 1.1), https://doi.org/10.1594/WDCC/NSBClim_v1.1, 2017.
- Holt, J., Butenschön, M., Wakelin, S. L., Artioli, Y., and Allen, J. I.: Oceanic controls on the primary production of the northwest European continental shelf: model experiments under recent past conditions and a potential future scenario,
- 545 *Biogeosciences*, 9, 97–117, <https://doi.org/10.5194/bg-9-97-2012>, 2012.



- Holt, J., Schrum, C., Cannaby, H., Daewel, U., Allen, I., Artioli, Y., Bopp, L., Butenschon, M., Fach, B. A., Harle, J., Pushpadas, D., Salihoglu, B., and Wakelin, S.: Potential impacts of climate change on the primary production of regional seas: A comparative analysis of five European seas, *Prog. Oceanogr.*, 140, 91–115, <https://doi.org/10.1016/j.pocean.2015.11.004>, 2016.
- 550 Holt, J., Polton, J., Huthnance, J., Wakelin, S., O’Dea, E., Harle, J., Yool, A., Artioli, Y., Blackford, J., Siddorn, J., and Inall, M.: Climate-Driven Change in the North Atlantic and Arctic Oceans Can Greatly Reduce the Circulation of the North Sea, *Geophys. Res. Lett.*, 45, 11,827–11,836, <https://doi.org/10.1029/2018GL078878>, 2018.
- Holt, J., Harle, J., Wakelin, S., Jardine, J., and Hopkins, J.: Why Is Seasonal Density Stratification in Shelf Seas Expected to Increase Under Future Climate Change?, *Geophys. Res. Lett.*, 49, <https://doi.org/10.1029/2022GL100448>, 2022.
- 555 Jolliff, J. K., Kindle, J. C., Shulman, I., Penta, B., Friedrichs, M. A. M., Helber, R., and Arnone, R. A.: Summary diagrams for coupled hydrodynamic-ecosystem model skill assessment, *J. Mar. Syst.*, 76, 64–82, <https://doi.org/10.1016/j.jmarsys.2008.05.014>, 2009.
- Jones, C. D., Hughes, J. K., Bellouin, N., Hardiman, S. C., Jones, G. S., Knight, J., Liddicoat, S., O’Connor, F. M., Andres, R. J., Bell, C., Boo, K.-O., Bozzo, A., Butchart, N., Cadule, P., Corbin, K. D., Doutriaux-Boucher, M., Friedlingstein, P.,
- 560 Gornall, J., Gray, L., Halloran, P. R., Hurtt, G., Ingram, W. J., Lamarque, J.-F., Law, R. M., Meinshausen, M., Osprey, S., Palin, E. J., Parsons Chini, L., Raddatz, T., Sanderson, M. G., Sellar, A. A., Schurer, A., Valdes, P., Wood, N., Woodward, S., Yoshioka, M., and Zerroukat, M.: The HadGEM2-ES implementation of CMIP5 centennial simulations, *Geosci. Model Dev.*, 4, 543–570, <https://doi.org/10.5194/gmd-4-543-2011>, 2011.
- Kay, S., McEwan, R., and Ford, D.: North West European Shelf Production Centre
- 565 NWSHELF_MULTIYEAR_BIO_004_011 quality information document, Copernicus Marine Environment Monitoring Service, 2020.
- Kearney, K. A., Bograd, S. J., Drenkard, E., Gomez, F. A., Haltuch, M., Hermann, A. J., Jacox, M. G., Kaplan, I. C., Koenigstein, S., Luo, J. Y., Masi, M., Muhling, B., Pozo Buil, M., and Woodworth-Jefcoats, P. A.: Using Global-Scale Earth System Models for Regional Fisheries Applications, *Front. Mar. Sci.*, 8, 622206, <https://doi.org/10.3389/fmars.2021.622206>,
- 570 2021.
- Keeling, C. D., Piper, S. C., Bacastow, R. B., Wahlen, M., Whorf, T. P., Heimann, M., and Meijer, H. A.: Exchanges of Atmospheric CO₂ and ¹³CO₂ with the Terrestrial Biosphere and Oceans from 1978 to 2000. I. Global Aspects, 29, 2001.
- Kwiatkowski, L., Torres, O., Bopp, L., Aumont, O., Chamberlain, M., Christian, J. R., Dunne, J. P., Gehlen, M., Ilyina, T., John, J. G., Lenton, A., Li, H., Lovenduski, N. S., Orr, J. C., Palmieri, J., Santana-Falcón, Y., Schwinger, J., Séférian, R.,
- 575 Stock, C. A., Tagliabue, A., Takano, Y., Tjiputra, J., Toyama, K., Tsujino, H., Watanabe, M., Yamamoto, A., Yool, A., and Ziehn, T.: Twenty-first century ocean warming, acidification, deoxygenation, and upper-ocean nutrient and primary production decline from CMIP6 model projections, *Biogeosciences*, 17, 3439–3470, <https://doi.org/10.5194/bg-17-3439-2020>, 2020.
- Legendre, P. and Legendre, L.: *Numerical Ecology*, 3rd ed., Elsevier, 990 pp., 2012.



- 580 Madec, G., Romain, B.-B., Jérôme, C., Emanuela, C., Andrew, C., Christian, E., Doroteaciro, I., Dan, L., Claire, L., Tomas, L., Nicolas, M., Sébastien, M., Silvia, M., Clément, R., Dave, S., Martin, V., Simon, M., George, N., Mike, B., and Guillaume, S.: NEMO ocean engine, , <https://doi.org/10.5281/zenodo.3878122>, 2019.
- O’Dea, E., Furner, R., Wakelin, S., Siddorn, J., While, J., Sykes, P., King, R., Holt, J., and Hewitt, H.: The CO₂ configuration of the 7 km Atlantic Margin Model: large-scale biases and sensitivity to forcing, physics options and vertical resolution, *Geosci. Model Dev.*, 10, 2947–2969, <https://doi.org/10.5194/gmd-10-2947-2017>, 2017.
- 585 O’Dea, E. J., Arnold, A. K., Edwards, K. P., Furner, R., Hyder, P., Martin, M. J., Siddorn, J. R., Storkey, D., While, J., Holt, J. T., and Liu, H.: An operational ocean forecast system incorporating NEMO and SST data assimilation for the tidally driven European North-West shelf, *J. Oper. Oceanogr.*, 5, 3–17, <https://doi.org/10.1080/1755876X.2012.11020128>, 2012.
- Oschlies, A., Duteil, O., Getzlaff, J., Koeve, W., Landolfi, A., and Schmidtko, S.: Patterns of deoxygenation: sensitivity to natural and anthropogenic drivers, *Philos. Trans. R. Soc. Math. Phys. Eng. Sci.*, 375, 20160325, <https://doi.org/10.1098/rsta.2016.0325>, 2017.
- 590 Oschlies, A., Brandt, P., Stramma, L., and Schmidtko, S.: Drivers and mechanisms of ocean deoxygenation, *Nat. Geosci.*, 11, 467–473, <https://doi.org/10.1038/s41561-018-0152-2>, 2018.
- OSPAR: Integrated report 2003 on the eutrophication status of the OSPAR maritime area based upon the first application of the comprehensive procedure, OSPAR Commission, London, UK, 2003.
- 595 Riahi, K., Grübler, A., and Nakicenovic, N.: Scenarios of long-term socio-economic and environmental development under climate stabilization, *Technol. Forecast. Soc. Change*, 74, 887–935, <https://doi.org/10.1016/j.techfore.2006.05.026>, 2007.
- Ricker, M. and Stanev, E. V.: Circulation of the European northwest shelf: a Lagrangian perspective, *Ocean Sci.*, 16, 637–655, <https://doi.org/10.5194/os-16-637-2020>, 2020.
- 600 Smyth, T. J., Moore, G. F., Hirata, T., and Aiken, J.: Semianalytical model for the derivation of ocean color inherent optical properties: description, implementation, and performance assessment, *Appl. Opt.*, 45, 8116, <https://doi.org/10.1364/AO.45.008116>, 2006.
- Taylor, K. E., Stouffer, R. J., and Meehl, G. A.: An Overview of CMIP5 and the Experiment Design, *Bull. Am. Meteorol. Soc.*, 93, 485–498, <https://doi.org/10.1175/BAMS-D-11-00094.1>, 2012.
- 605 Tinker, J., Lowe, J., Pardaens, A., Holt, J., and Barciela, R.: Uncertainty in climate projections for the 21st century northwest European shelf seas, *Prog. Oceanogr.*, 148, 56–73, <https://doi.org/10.1016/j.pocean.2016.09.003>, 2016.
- Verberk, W. C. E. P., Atkinson, D., Hoefnagel, K. N., Hirst, A. G., Horne, C. R., and Siepel, H.: Shrinking body sizes in response to warming: explanations for the temperature–size rule with special emphasis on the role of oxygen, *Biol. Rev.*, 96, 247–268, <https://doi.org/10.1111/brv.12653>, 2021.
- 610 Vörösmarty, C. J., Fekete, B. M., Meybeck, M., and Lammers, R. B.: Global system of rivers: Its role in organizing continental land mass and defining land-to-ocean linkages, *Glob. Biogeochem. Cycles*, 14, 599–621, <https://doi.org/10.1029/1999GB900092>, 2000.

<https://doi.org/10.5194/egusphere-2023-1049>

Preprint. Discussion started: 31 May 2023

© Author(s) 2023. CC BY 4.0 License.



- 615 Wakelin, S. L., Artioli, Y., Holt, J. T., Butenschön, M., and Blackford, J.: Controls on near-bed oxygen concentration on the Northwest European Continental Shelf under a potential future climate scenario, *Prog. Oceanogr.*, 187, 102400, <https://doi.org/10.1016/j.pocean.2020.102400>, 2020.
- Yool, A., Popova, E. E., and Coward, A. C.: Future change in ocean productivity: Is the Arctic the new Atlantic?, *J. Geophys. Res. Oceans*, 120, 7771–7790, <https://doi.org/10.1002/2015JC011167>, 2015.
- Young, E. F. and Holt, J. T.: Prediction and analysis of long-term variability of temperature and salinity in the Irish Sea, *J. Geophys. Res.*, 112, C01008, <https://doi.org/10.1029/2005JC003386>, 2007.